Chemical Engineering Journal xxx (xxxx) 155957

Contents lists available at ScienceDirect

Chemical Engineering Journal

journal homepage: www.elsevier.com/locate/cej

Biodegradation of thermoplastic starch by a newly isolated active microbial community: Deciphering the biochemical mechanisms controlling bioprocess robustness

Evdokia Syranidou [a, 1], Fryni Pyrilli [a, 1], Athanasios Fountoulakis [b], Georgios Constantinides [c], Nicolas Kalogerakis [b], Michalis Koutinas [a, *]

[a] Department of Chemical Engineering, Cyprus University of Technology, Limassol, Cyprus
[b] Department of Chemical and Environmental Engineering, Technical University of Crete, Chania, Greece
[c] Department of Mechanical Engineering and Materials Science and Engineering, Cyprus University of Technology, Cyprus

ARTICLE INFO

Keywords:
Bioplastics
Thermoplastic starch
Aerobic biodegradation
Soil community
Biofilm dynamics

ABSTRACT

Defining sustainable end-of-life routes for bioplastics comprises a task of outmost importance, while biological recycling constitutes the most favorable option for several biopolymers, such as thermoplastic starch (TPS). To our knowledge, this is the first study to assess the biodegradation of TPS pellets and films in aqueous cultures employing an acclimated microbial community. Biological treatment of bioplastics displayed a two-phase pattern that included different biodegradation rates, where TPS removal in the first phase remained high and decelerated in the second phase reaching a plateau. Thus, TPS weight reduction of 14.8 % was observed using pellets following 10 d of incubation, while although films exhibited higher reduction (slightly over 30 % in 15 d), the biodegradation rate was significantly reduced thereafter. Several changes of starch related bands were detected (using FTIR) in the surface of both pellets and films during the bioprocess, indicating induction of a common biodegradation pathway. Distinct bacterial assemblages were formed during the TPS biodegradation process and statistically significant differences were detected in the abundance of several genera between the two degradation phases. Fungal communities were more stable (*Fusarium* and *Neocosmospora* were dominant at all times) and there was no effect of biofilm or degradation phase on fungal community composition. Overall, a more diverse community incorporating lower catalytic activity was gradually formed, as confirmed by the shift between k-stategist and r-stategist taxa monitored, while crystalline over amorphous regions were enhanced in the biopolymer during TPS biodegradation, responses consistent with the biodegradation rate reduction observed in the plateau stage. The study highlighted the biochemical mechanism limiting TPS biodegradation processes and the significant potential of the newly isolated community in the development of TPS waste treatment technologies.

1. Introduction

Although plastics comprise part of our everyday life, their high overuse comes at a tremendous environmental cost. More than 400 million t of plastics are produced globally every year, while approximately 40 % of plastics in Europe are used for packaging [1]. Linear production of plastics and lack of efficient waste management result in the release of billion t of plastic into the environment, which eventually end up in the marine and soil ecosystems [2]. Although increasing the durability of plastics could improve their performance the specific approach poses a serious environmental threat by rendering these materials resistant to natural degradation. Accumulated plastics could be fragmented into smaller particles, gradually forming microplastics or even nanoplastics [3] that enter the food chain from the lowest trophic level

Abbreviations: ATR-FTIR, Attenuated total reflection – Fourier transform infrared spectroscopy; EOL, end-of-life; GHG, greenhouse gas; GMO, Genetically modified organism; KEGG, Kyoto Encyclopedia of Genes and Genomes; LCA, Life Cycle Analysis; LDPE, Low-density polyethylene; NMDS, Non-metric multidimensional scaling; PBAT, polybutylene adipate terephthalate; PCL, polycaprolactone; PHAs, polyhydroxyalkanoates; PLA, polylactic acid; SEM, Scanning electron microscopy; TPS, thermoplastic starch; TOC, total organic carbon

* Corresponding author.
E-mail address: michail.koutinas@cut.ac.cy (M. Koutinas).

[1] These authors contributed equally to this work.

https://doi.org/10.1016/j.cej.2024.155957
Received 17 June 2024; Received in revised form 25 August 2024; Accepted 17 September 2024
1385-8947/

(plankton) and travel up food chain to species consumed by humans impacting on human and animal health [4]. Thus, alternative waste management systems must be proposed and implemented.

Bioplastics arise as promising alternative materials for substitution of their fossil-based counterparts [5], which could potentially alleviate the pressure that conventional plastics pose to the environment. Bioplastics are characterised as environmental friendly and non-toxic, contributing significantly towards achieving the transition to circular bioeconomy [6], reducing greenhouse gas (GHG) emissions by up to 225 % compared to conventional plastics [7]. Currently, almost every conventional plastic has its own alternative bioplastic, while the overall production of biobased/non-biodegradable and biodegradable plastics was projected to grow reaching 2.8 million t in 2025 [8]. Therefore, establishing waste management strategies for bioplastics aiming to avoid pollution problems similar to those caused by conventional plastics is required, given that not all bioplastics are biodegradable under natural environmental conditions [9]. Existing end-of-life (EOL) options for bioplastics include a range of technologies such as mechanical recycling, anaerobic digestion, aerobic biodegradation in soil and composting [10]. Although industrial composting (EN 13432) constitutes the predominant end-of-life option for bioplastics, the specific treatment could be only effective under certain environmental conditions, necessitating prolonged processing periods and elevated temperatures [11], while resulting in accumulation of residues [12]. Moreover, the degradation rates of food waste and bioplastics in composting processes are different and a fraction of the polymers should be frequently landfilled. Thus, bioplastics do not meet the USDA's National Organic Program's standards and therefore it was proposed developing two separate waste streams (bioplastic collection infrastructure and composting) [13]. Composting is not considered as a fully circular option given that new feedstock is required for the synthesis of biopolymers [14], while mechanical recycling of biodegradable plastics has not been operated at industrial scale yet [15]. Thus, an urgent need exists towards development of sustainable EOL strategies for biodegradable bioplastics aiming to meet the growing industrial demand for reduction of non-renewable resource consumption, establishment of sustainable bioeconomics and dealing with the high production cost entailed.

Biological recycling utilizing microorganisms rather than chemicals for the depolymerization process constitutes a viable technology for the management of bioplastics such as polyhydroxyalkanoates (PHAs) and thermoplastic starch (TPS) [16]. TPS comprises an emerging biopolymer and starch, the main constituent of TPS, is abundant, cheap and easy to produce. The specific bioplastic is characterised as both biobased and biodegradable [9], while TPS applications range in various sectors including packaging, food, textile, pharmaceutical and agricultural industries [17]. Several microorganisms hold the capacity to degrade TPS in diverse environments including soil, compost and anaerobic digestion [18,19]. Thus, TPS degraded completely within 136 d in soil consisting 70 % industrial quartz sand, 10 % kaolinite clay, 16 % natural soil and 4 % mature compost [20], while composting trials aiming to biodegrade TPS/PLA blends and their constituents for 90 d demonstrated 87 % removal of TPS films at 58 °C [21]. Aerobic biodegradation proceeds in soil and composting environments via a highly diverse microbial community, which acts with the aid of enzymes [22]. The fungus *Aspergillus oryzae* and bacterial strains including *Bacillus circulans*, *Klebsiella pneumonica* and *Bacillus stearothermophilus* have been reported to produce a variety of starch degrading enzymes [23].

Although the treatment of TPS using soil microorganisms could be effective, the process proceeds via use of thermophilic conditions. Thus, the biodegradation of TPS in liquid cultures has not yet been explored enabling the use of mesophilic temperatures, which could potentially set the basis for bioprocess cost reduction. Considering that the EOL options for biopolymers could alter the product's environmental profile, since the cost of industrial composting and disposal transportation may prove bioplastics to incorporate higher global warming potential if EOL is considered during LCA analysis [13], the development of sustainable EOL strategies should be carefully considered. The biodegradation of TPS in liquid cultures at mesophilic temperatures can lay the foundations for TPS waste treatment in systems different than composting, potentially reducing release of harmful emissions and accumulation of microplastic residues. Thus, the aim of the current study was to conduct the preliminary steps required to develop a sustainable bioprocess for TPS removal using aqueous cultures via isolation of the biofilm community formed on TPS exposed to agricultural soil and assess its catabolic activity during the biodegradation of TPS films and pellets. Several parameters in terms of polymer characteristics (e.g. FTIR-ATR and SEM analysis) and biofilm community composition (16S rRNA gene and ITS2 ribosomal region sequencing) were monitored to verify TPS degradation and elucidate the underling mechanisms of the process.

2. Materials and methods

2.1. Materials and chemicals

The TPS pellets and films (BIOPLAST GF 106/02) used in the experiments were produced by BIOTEC (Rhein, Germany) and were kindly provided by PLASTIKA FARSALON (Larissa, Greece). The biomaterial comprised plasticizer-free and GMO-free thermoplastic containing natural potato starch and included pellets of cylindrical shape with approximate height of 3 mm as well as 1.25 kg cm^{-3} density. The surface area of films comprised 1 cm^2. All chemicals used were acquired from Sigma-Aldrich Ltd. Company (Dorset, UK) and were of analytical grade.

2.2. Soil microcosm experiment and enrichment culture

Composite soil samples applied in the soil experiment, were collected at a depth of 0–10 cm from an agricultural field planted with tomato plants located in Falasarna (Crete, Greece). The soil was air-dried and sieved through a 2 mm sieve. Glass vases (1 L) were used in triplicate and they were filled with gravel (100 g added at the bottom of glass vases) followed by 500 g of air-dried soil samples. TPS pellets were placed at a depth of 2–10 cm at a concentration of 0.1 % (w/w), while the initial soil moisture was 5 %. The experiment was conducted at TUC campus (Chania, Greece) and maintained for at least 220 d (March 2022 to November 2022). The soil moisture was kept at 5 %, while 3 vases were permanently removed at specific time intervals to determine the extent of weight reduction and biofilm development on the surface of the pellets as described in Section 2.4.

The microbial community isolated from TPS pellets following 220 d of soil microcosms incubation was used in the enrichment experiment, while the experimental design followed is presented in Figure S1. Briefly, TPS pellets were collected from the soil and the biofilm formed on the surface of the pellets was removed as described in Section 2.3 and used in the enrichment culture. Approximately 1 % (v/v) biofilm solution was transferred to mineral minimum medium consisted of 2 g L^{-1} NaH_2PO_4, 0.5 g L^{-1} $MgSO_4{\cdot}7H_2O$, 0.2 g L^{-1} KH_2PO_4 and 1 g L^{-1} yeast extract [24] as well as sterile TPS pellets (5 g L^{-1}). Every 10 d, 1 % (v/v) inoculum and TPS pellets with plastisphere were transferred to fresh media. The experiment was maintained for at least 3 months under mesophilic (30 °C) conditions in 250 mL flasks using 100 mL mineral minimum medium under shaking at 120 rpm.

2.3. TPS biodegradation experiments

The microbial community developed on the surface of TPS pellets at the end of the enrichment period was further used in the degradation experiments conducted constituting the seed community. TPS pellets and films were surface sterilized prior use by immersion in ethanol solution and subsequently dried for 24 h at 30 °C. Experiments were car-

ried out under mesophilic (30 °C) conditions in 250 mL flasks in triplicate using 100 mL mineral minimum medium, inoculum of the seed biofilm community (initial concentration: 10^6 cells mL^{-1}) and TPS pellets/films (5 g L^{-1}). The mineral minimum medium consisted 2 g L^{-1} NaH_2PO_4, 0.5 g L^{-1} $MgSO_4{\cdot}7H_2O$, 0.2 g L^{-1} KH_2PO_4 and 1 g L^{-1} yeast extract [24]. At each sampling day, 3 flasks were permanently removed. The biofilm was harvested by adding bioplastic particles in sterile distilled water supplemented with 3 drops of Tween^{80}. The solution that included the particles was left overnight under shaking. Subsequently, pellets or films were removed and the solution was considered as "biofilm", while the pellets/films were considered as clean. In control cultures, only the sterile TPS pellets/films were added in the medium to assess the extent of abiotic hydrolysis.

2.4. Analyses

2.4.1. TPS weight, total organic carbon content and biofilm determination

The biofilm of pellets/films was collected at the end of each experiment as described in section 2.3 and stored for further analysis at −20 °C. Clean pellets/films were dried in an oven at 40 °C. The weight of the bioplastic was determined employing 4-decimal point accuracy and the percentage of weight reduction was calculated using the following equation:

$$Weight\ reduction\ (\%) = (mi - mf)\ /mi \times 100$$

where mi and mf correspond to the initial and final mass of TPS respectively.

Aqueous culture samples were withdrawn and filtered using 0.2 μm filters and non-purgeable organic carbon was determined by catalytic combustion at high temperature using total organic carbon (TOC) analyzer (TOC-LCPH/CPN, Shimadzu, Kyoto, Japan). Biofilm attachment was confirmed by staining the surface of 3 pellets using Crystal Violet (1 % aqueous solution, Sigma-Aldrich) as previously described [25].

2.4.2. Attenuated total reflection – Fourier transform infrared spectroscopy (ATR-FTIR)

The chemical structure of pellet/film surfaces was assessed over time in the cultures performed by studying the functional groups entailed using attenuated total reflection – Fourier-transform infrared spectroscopy (ATR-FTIR). Analyses were performed on a Nicolet™ iS50 FTIR Spectrometer equipped with a diamond ATR accessory (Thermo Scientific, USA). Spectra were obtained using Thermo Scientific's OMNIC software, while five clean pellets per treatment were assessed in each replicate. Spectrum acquisition was conducted following 32 scans for absorbance numbers between 4000 and 400 cm^{-1}, with a scan resolution of 4 cm^{-1}. The carbonyl and starch index were calculated as previously described [26], while the ratio of amorphous/crystalline region was additionally assessed [27].

2.4.3. Scanning electron microscopy (SEM)

The effects of biodegradation and biofilm formation on the surface of the biomaterial was investigated using a Scanning Electron Microscope (Quanta 200, FEI, Hillsboro, OR, USA) using 20 kV acceleration voltage and 10 mm working distance. All samples were sputter coated with a thin (~10 nm) film of gold prior to the investigation in order to enhance surface conductivity and avoid charging effects. Biofilm fixation on pellets was achieved by washing twice with 2 % (w/v) aqueous sodium dodecyl sulphate solution for 30 min under mild shaking followed by rinsing with distilled water. Samples were immersed in 70 % (v/v) ethanol solution for 20 min and left for air-drying overnight. The plastic pieces were washed using 0.1 M phosphate buffer (pH 7.2) for 20 min and fixed with 2 % (v/v) formaldehyde for 2 h under shaking, aiming to observe the developed biofilm on the surface of TPS. Subsequently, samples were dehydrated by immersion into a graded series of ethanol solutions for 30 min each (25 %, 50 %, 75 % and 90 % v/v) and left to dry.

2.4.4. Flow cytometry

The number of cells attached to the plastisphere was quantified using flow cytometry. Cells forming the biofilm were harvested by adding bioplastic particles in sterile distilled water supplemented with 3 drops of Tween^{80} and stirred employing a magnetic stirrer operated at 150 rpm. Bioplastic particles were removed and the remaining solution contained the cells that constituted the biofilm as a suspended culture. A given volume of the solution was fixed with glutaraldehyde (final concentration of 2 % v/v) for at least 2 h at 4 °C. Fixed samples were stained with 2 μL of 1X Thiazole Green (10,000X Biotium) and incubated in the dark for 20 min prior analysis using a Beckman-Coulter CytoFLEX flow cytometer. Samples were processed at a flow rate of 30 μL min^{-1} and the measurement was terminated upon recording of 10.000 events was established. A blank sample of 998 μL of the media stained with 2 μL of 1X Thiazole Green was used to eliminate background noise.

2.4.5. High-throughput sequencing and data processing

DNA was extracted from the biofilm using the DNeasy PowerSoil® DNA Kit from QIAGEN (Hilden, Germany) according to the manufacturer's instructions. The V3-V4 regions of the 16S rRNA gene and the ITS2 ribosomal region were sequenced for bacterial and fungal communities. Sequencing was performed in 3 biological replicates using an Illumina NovaSeq PE250 (2 × 250 bp) system by Novogene (UK) Company Ltd. (Cambridge, UK). The following primers were used as forward and reverse respectively, aiming to amplify the V3-V4 region of 16S: 341F (5′-CCTAYGGGRBGCASCAG-3′) 806R (5′-GGACTACNNGGGTATCTAAT-3′). The ITS2 region was amplified using ITS3 (5′-GCATCGATGAAGAACGCAGC-3′) and ITS4 (5′-TCCTCCGCTTATTGATATGC-3′). Sequence data can be found in NCBI's Sequence Read Archive under the accession no. PRJNA1068809.

Raw sequence reads were trimmed using cutadapt v3.7 to remove primer DNA sequences [28], with no primer mismatch allowed. The bioinformatics analysis was performed in R version 4.3.1 (R Core Team, 2021). The DADA2 pipeline was employed to merge, denoise and dereplicate the sequences into amplicon sequence variants (ASVs) using the package dada2 [29]. Each ASV was classified according to the Silva 138 database [30] for the 16S rRNA region and UNITE database [31] for the ITS2 region. The DECIPHER R package [32] was used for multiple amplicon sequence variant (ASV) alignment and the phangorn R package version 2.8.1 [33] was used for the construction of a phylogenetic tree.

The package microeco v1.3.0 was used for the downstream analysis [34]. 16S rRNA gene sequences assigned to chloroplasts and mitochondria were removed. Aiming to investigate the alpha diversity of microbial communities, indices were calculated for Shannon diversity, Simpson evenness and observed number of taxa. ANOVA was performed to determine whether case assumptions for normality and heterogeneity are met according to Levene's and Shapiro-Wilk's tests or Kruskal-Wallis and to assess the significance of observed differences. The beta diversity analysis was investigated through non-metric multidimensional scaling (nMDS) using the Bray-Curtis distance with the R package vegan [35]. Pairwise PERMANOVA (999 permutations) using the Bray-Curtis distance was carried out to determine the statistical significance among polymer shape, time and biofilm phase. Subsequently, the homogeneity of group dispersions (variances) was tested (PERMDISP). The significant bioindicator taxa across groups were identified using Linear discriminant analysis Effect Size (LEfSe) [36]. Metastats analysis was used to detect significantly differential bacteria at genus level among groups [37]. Metabolic function prediction for the bacterial communities was performed using Tax4Fun2 [38]. Data analysis, statis-

tics, and plotting in R further included the following packages: phyloseq [39] and ggplot2.

2.4.6. Secondary microplastics assessment

A fraction of the aqueous media was mixed with an oversaturated solution of $CaCl_2$ (~1.44 g mL^{-1}) to extract the secondary microplastics by density separation [40]. The solution was mixed using a shaker overnight and subsequently allowed to settle on the bench. Several droplets of the supernatant were stained employing Nile red [41] and the concentration of microplastics was determined using a fluorescence microscope (Leica DMLB microscope, Leica Microsystems, Wetzlar, Germany).

3. Results and discussion

3.1. Isolation of a soil plastisphere community for TPS biodegradation

Polymers incorporating natural structures, such as starch-based plastics, are considered highly susceptible to microbial degradation, especially within the soil environment. Thus, virgin TPS pellets were incubated in agricultural soil for 220 d, aiming to isolate a microbial community holding the desired metabolic traits towards TPS detoxification. Upon exposure to agricultural soil, the biodegradation process of TPS pellets displayed a two-phase pattern that included different removal rates (Fig. 1A). In the first phase (0–50 d) the biodegradation rate monitored was high and significantly ($p < 0{,}001$) decelerated in the second phase (50–220 d). During the first 20 d, the weight of TPS decreased by 12 % and the removal reached 33 % at 50 d. Subsequently, biodegradation of the biopolymer was substantially reduced given that 49 % weight reduction was exhibited following 220 d of exposure. Biofilm development on the surface of pellets followed a similar pattern, where a steep increase was observed during the first 50 d followed by establishment of a plateau in the biofilm's specific biomass concentration. Similarly to the results obtained in the current work, a three phase degradation process has been demonstrated upon TPS and starch incubation under controlled composting conditions [42,43]. The lag phase ranged from 0 to 2 days which was also observed in the current study. The biodegradation phase lasted from day 3 to day 25, while the overall degradation was 73 % following 56 days at 58 °C based on the CO_2 released [42]. However, high variation in the degradation rate of TPS (including starch blends) has been demonstrated in the soil environment, where different degradation tests exhibited a median of 80 % removal [44].

The FTIR spectra of virgin TPS pellets as well as following exposure to agricultural soil displayed significant differences during the experiment (Figure S2). The hydroxyl band (3200 – 3300 cm^{-1}) present in the spectrum of the virgin polymer completely disappeared following 220 d of exposure. The specific band was ascribed either to the stretching vibrations of the hydroxyl (OH) groups of the starch glucose unit or those of the plasticizer [45]. Moreover, variations were detected in the spectra that ranged between 1100 and 1000 cm^{-1}, which could be attributed to C–O stretching [46], while weakening or breaking of the bonds was additionally supported by the FTIR spectra obtained.

3.2. Weight reduction and biofilm development in degradation experiments

The biofilm community formed on TPS pellets at 220 d was isolated and further used in biodegradation experiments conducted in shake flasks using two different polymer shapes following a prolonged enrichment period. Increased weight reduction rate was monitored upon pellets incubation with the acclimated microbial community as compared to soil. A weight reduction of 14.8 % ± 0.3 in 10 d was observed, which was subsequently reduced to additional reduction of approximately 2 % per week thereafter (Fig. 1B). Thus, a degradation rate of

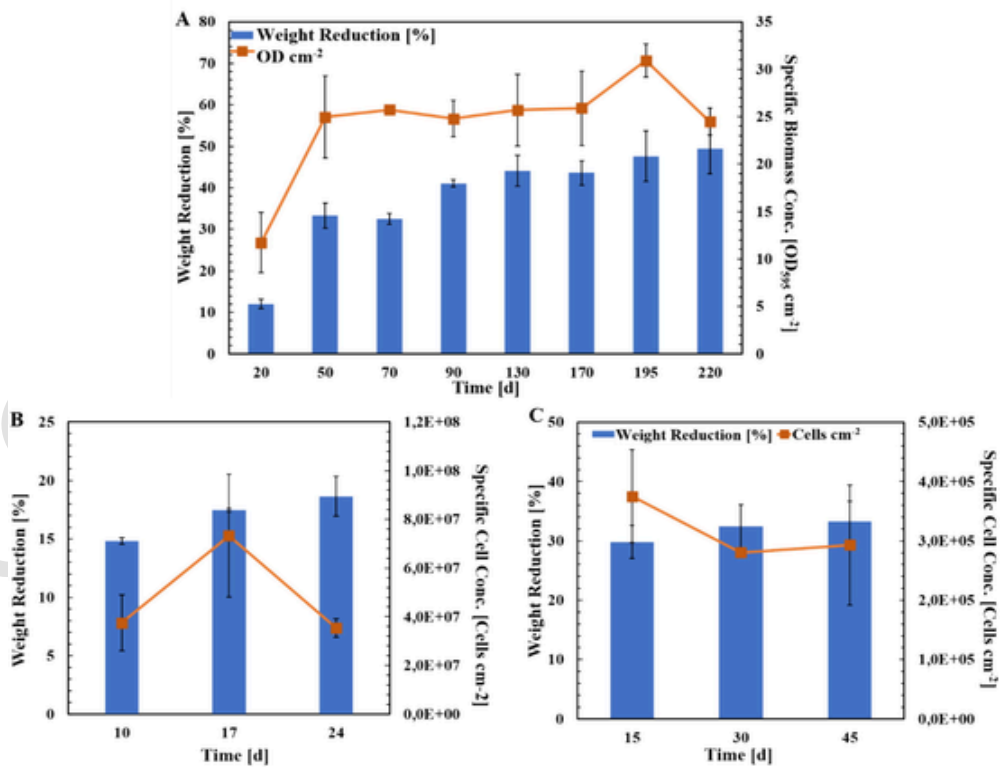

Fig. 1. Weight reduction (%) and biofilm development (specific biomass concentration) on (A) TPS pellets exposed to agricultural soil. Moreover, weight reduction and biofilm development by aqueous cultures of the microbial community isolated on (B) TPS pellets and (C) films was monitored.

5.8 mg d^{-1} was observed for the first 10 d, which was further reduced to 3.7 mg d^{-1} and 1.7 mg d^{-1} until the end of the experiment. The cell concentration of the biofilm established was increased by 64 % between 10 and17 d reaching 7 × 10^7 cells cm^{-2}. However, although the specific cell number dropped significantly by 52 % following 24 d of incubation, cell abundance remained at high levels. Similarly to the biodegradation pattern monitored in the soil environment, the process conducted at aqueous cultures followed a two-phase mode that included distinct biodegradation rates, while the plateau phase started at 17 d. Cultures performed employing TPS films exhibited significant weight reduction, which reached slightly over 30 % at 15 d, while 3 % additional weight reduction was monitored until 45 d (Fig. 1C). Biodegradation of TPS films has shown that the plateau stage could be reached at 100 d during incubation at 28 °C [47]. Moreover, the biodegradation process of starch could follow an asymptotic curve, where a significant fraction of the biopolymer is removed within 3 d following entry in soil, while the rest of its mass could remain for weeks or even years [48]. During TPS production the natural granular shape and crystalline structure of starch are lost and usually a plasticizer is added. As a result, various TPS degradation rates have been reported in soil and composting experiments, ranging from complete removal within 6 months to complete absence of weight loss following 100 d of burial [23].

The extent of TPS mineralization in the liquid medium was additionally assessed through TOC analysis. A significant part of the TPS weight loss was potentially transformed to CO_2 and microbial biomass considering that TOC concentrations remained always substantially lower as compared to those expected in the hypothetical case that no mineralization occurred. The mineral medium (in the absence of bioplastics and cells) included 378 mg L^{-1} TOC. Moreover, employing the weight loss of TPS following 10 d of incubation enabled calculating the maximum amount of carbon that could have dissolved in the biomedium which constituted an additional 255 mg L^{-1} TOC. Although the maximum theoretical TOC content was 633 mg L^{-1}, the TOC determined via biomedium sample analysis comprised 164 mg L^{-1} suggesting that 74 % of added carbon was removed, while carbon removal reached 80 % at 24 d. The remaining 20 % could be potentially attributed to the formation of secondary microplastics. In abiotic controls, TOC displayed an increasing trend along the course of the experiment, given that carbon was released from the pellets due to abiotic hydrolysis.

The material's shape constitutes a significant parameter affecting the biodegradation process. Thus, TPS weight reduction was enhanced by 10 % in films as compared to pellets. The specific effect could be attributed to the greater surface area exposed to degrading enzymes that act on the surface of the polymer using films as opposed to pellets [49]. Moreover, hydro-biodegradation is known to occur in hydrophilic polymers, such as starch and polyesters, incorporating preliminary abiotic or biotic hydrolysis followed by microbial assimilation [50]. Thus, due to the hydrophilic nature of TPS, non-enzymatic hydrolysis of the biopolymer occurred in the control experiments, where an average 9 % weight reduction of TPS due to hydrolysis was observed in all experiments.

3.3. ATR-FTIR and SEM analysis of TPS during biodegradation in microcosm experiments

3.3.1. ATR-FTIR analysis

Chemical changes on the surface of the biopolymer were studied using ATR-FTIR (Fig. 2). Both virgin forms of films and pellets incorporated the main characteristic peaks of the material including O-H

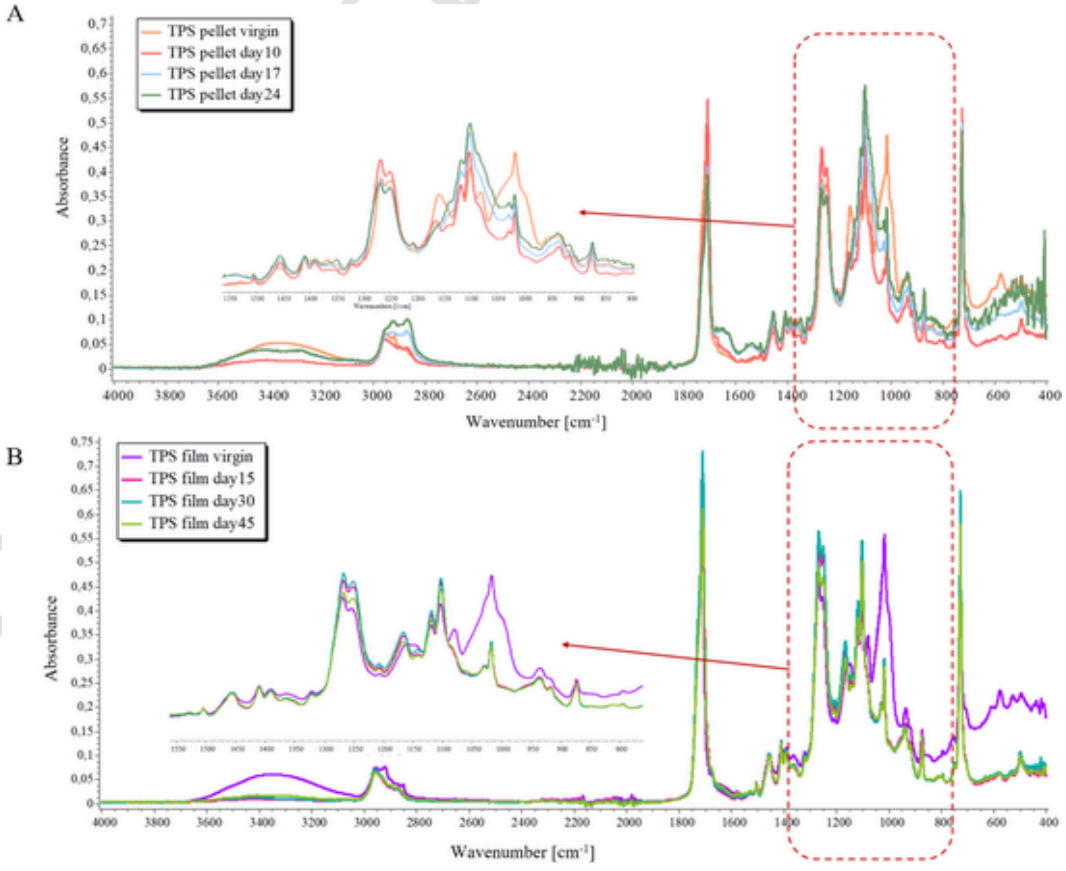

Fig. 2. The FTIR profiles of TPS (A) pellets and (B) films in microcosms.

(3200–3600 cm^{-1}) and C-H (2800–3000 cm^{-1}) stretches, C-C, C-O and C-O-C (950–1200 cm^{-1}) bending modes as well as skeletal mode vibration of the glycosidic linkage (900–950 cm^{-1}) [19,51]. During biodegradation by the isolated microbial consortium, several alterations such as narrowing/broadening of peaks, peak shifting or reduction of intensity were monitored indicating the weakening/breaking of bonds, which is aligned with the weight reduction of TPS monitored. The majority of alterations occurred in the so-called "fingerprint" characteristic peaks of starch, such as the vibrations of C-O-C bonds at 1155, 1087 and 1019 cm^{-1} as well as the peaks at 928, 862 and 764 cm^{-1} attributed to the pyranose ring [27]. Thus, the area in the range between 1020 and 1080 cm^{-1} was attributed to the C–O–C groups of starch [51] and displayed several modifications, such as peak disappearance or narrowing, in microbially treated pellets. Moreover, the band at 1160 cm^{-1}, which was assigned as a complex mode involving the CH_2OH side chain in amylose [52], gradually disappeared along the experiment. Changes were additionally observed in the absorption peak existing between 3000 and 2800 cm^{-1}, which correlates with the stretching of C–H bond. The bands located at 2929 cm^{-1} and 2945 cm^{-1} are characteristic of the C–H stretching vibration of amylose and amylopectin and they were not detected in TPS pellets exposed to the microbial community, supporting the degradation hypothesis. Similar modifications in the molecular structure have been previously demonstrated during TPS biodegradation in soil or compost environment [43,45]. Moreover, decrease of the peak at 1710 cm^{-1} attributed to the carbonyl group supports biological degradation.

Similar alterations were detected on the surface of TPS films exposed to the microbial community particularly in the area of 1020–1080 cm^{-1}, indicating that despite the higher weight reduction monitored in films as opposed to pellets a common biodegradation pathway could be potentially triggered. However, a number of differences were exhibited following biodegradation of pellets and films. Thus, the –OH stretching band in films disappeared following the biological treatment, potentially due to starch consumption while an increase in this band, which is usually assigned to the alcohol OH of the glucose residues [53] was observed in pellets along the degradation stages. Starch is enzymatically hydrolyzed to glucose via the extracellular enzymes α/β amylases secreted by bacteria and fungi, while biodegradation constitutes both surface and bulk phenomena [54]. Glucose is formed as soluble hydrolysis product, which is converted to pyruvic acid via glycolysis. Upon starch degradation to maltose (disaccharide) and glucose (monosaccharide), carbonyl groups are generated, while the subsequent opening of glucose β-D-glucopyranose ring leads to the formation of carboxylic and aldehyde groups, contributing to the increase of carbonyl peak [26]. The evolution of starch and carbonyl indices displayed opposite patterns (Fig. 3) in the case of films. Thus, the starch index progressively decreased and the carbonyl index increased (Fig. 3B), in fact this change was statistically significant ($p < 0.05$) for both indices within the first 15 d of the experiment. Statistically significant reduction of the starch index was also observed for pellets ($p < 0.05$). Concerning the order (amorphous versus crystalline region) of the polymers during degradation, the amorphous region could potentially decrease along the experimental period in both shapes (Fig. 3C-D), which could hamper the biodegradation rate. Specifically, more crystalline areas were detected in pellets following 24 d. In general, alterations of starch related bands were detected highlighting the effect of biodegradation on the polymer surface chemistry.

3.3.2. Determination of surface alterations via SEM analysis

The surface morphology of pellets and films at virgin state and during the experiment was observed using SEM analysis. The surface of pellets and films was irregular, but overall smooth without any holes or

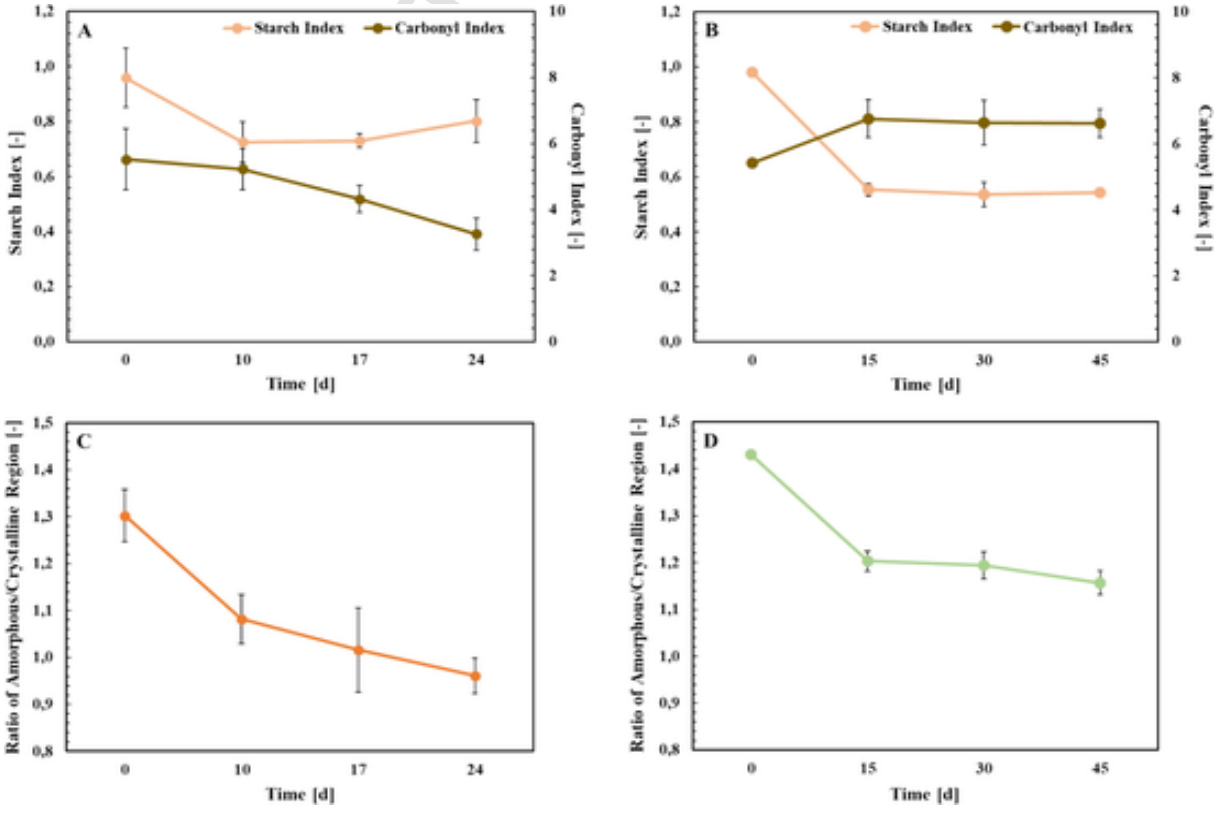

Fig. 3. The starch and carbonyl indices in TPS (A) pellets and (B) films and the ratio of amorphous versus crystalline regions of TPS (C) pellets and (D) films along the course of degradation.

cracks, while the microbial effect was evident on both polymer shapes (Fig. 4). Deep surface cracks were noticed on the surface of pellets at 10 d, while following 24 d of incubation surface morphology changed dramatically and a large number of extensive hyphae like structures were formed, in accordance with other studies [26]. Virgin films appeared to gradually lose their initial granular state, whereas a large number of cracks and voids were subsequently introduced on the surface. The granular state is usually observed due to the unresolved granular state of starch during the addition of plasticizers [51]. The surface morphology of films at 15 and 45 d were very similar, supporting the conclusion reached in Section 3.2 exhibiting that biodegradation reached a plateau following 15 d of treatment.

Biofilm formation was additionally monitored using SEM during the experiment as described in Fig. 4G-I. Approximately half of the pellet's surface area was covered, maintaining the rest of the surface accessible to microbial activity aiming to assess biofilm development on TPS over the course of the experiment. A dense biofilm network was formed that fully encaged the pellet at 17 d. The thickness of the biofilm ranged between 50 and 85 μm (the median thickness was 69 μm), while it slightly increased to 72 μm at 24 d, where the thickness ranged between 53 and 92 μm. Cracks were formed on the surface of the biofilm, while fragments of approximate thickness 30 μm were gradually detached. Filamentous fungi dominated the biofilm community and formed an interconnected structure where bacteria could be additionally observed, similarly to the biofilm structure previously reported for TPS biodegradation [21].

3.4. Secondary microplastics generation

Millions of microplastics and nanoplastics are generated upon exposure on traditional plastics in the natural ecosystems, posing a significant threat to the environment [55,56]. In fact, secondary micro/nanoplastics are considered as evidence of degradation and the process usually stops at the phase of fragmentation [49]. Moreover, biodegradable plastics undergo fragmentation into small particles during the biodegradation process, releasing a large number of micro/nanoplastics [57]. Thus, substantially elevated quantities of plastic fragments/particles were formed in simulated freshwater, estuarine and seawater natural habitats from polybutylene adipate terephthalate (PBAT) as compared to the use of low-density polyethylene (LDPE) [58]. Herein, more than 10^4 particles mL^{-1} mainly in fiber shape were quantified in the aqueous phase of microcosms using either pellets or films at all sampling points (Fig. 5). The concentration of secondary microplastics generated during the biodegradation of TPS pellets was stable. Moreover, a higher number of microparticles was produced during the first phase of biodegradation in TPS films, which decreased at the second phase, in accordance with TPS weight reduction.

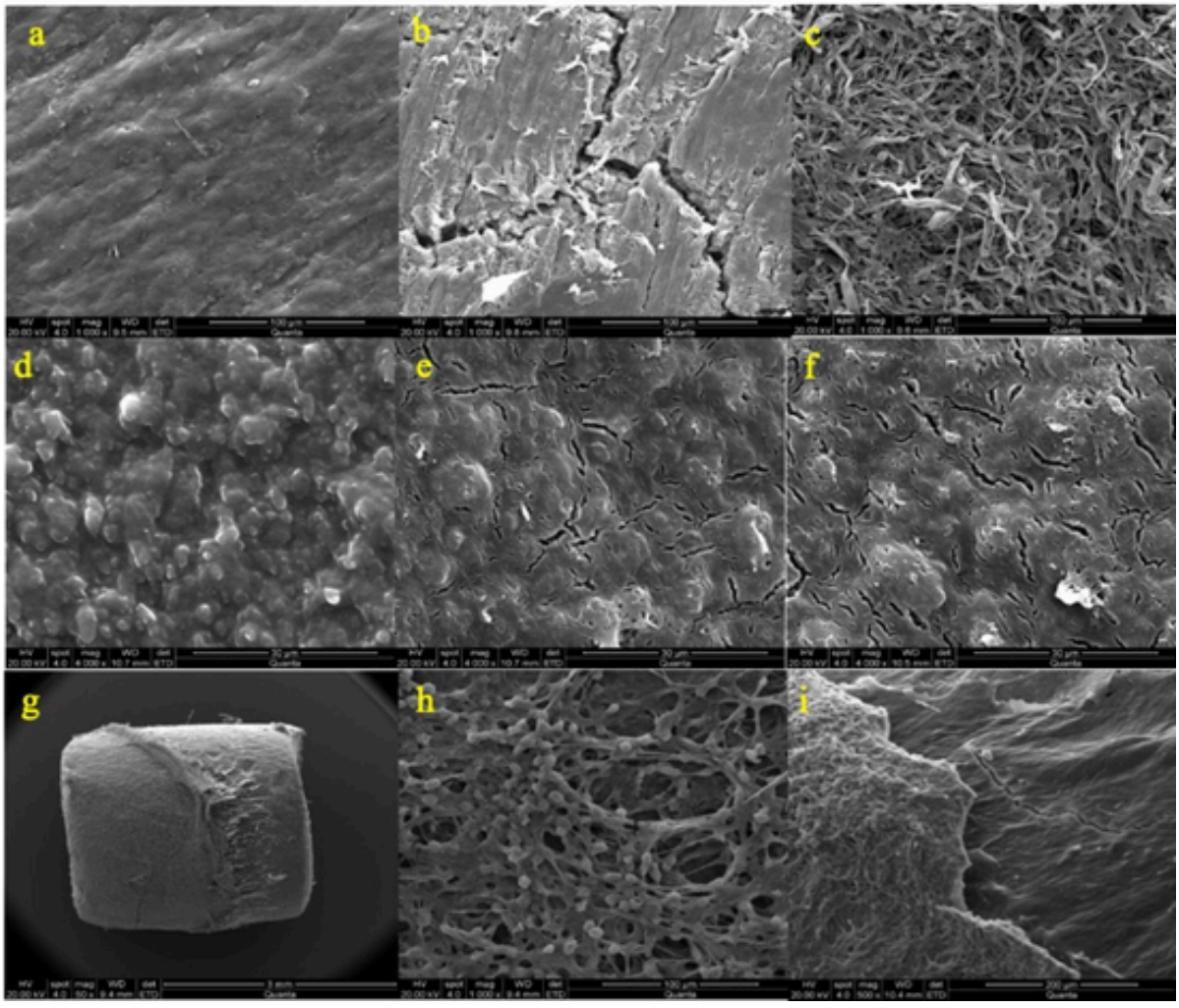

Fig. 4. SEM micrographs of (A) virgin TPS pellets, (B) TPS pellets at day 10, (C) TPS pellets at day 24, (D) virgin TPS films, (E) TPS films at day 15, (F) TPS films at day 45, (G-I) TPS pellet partially covered in half with biofilm.

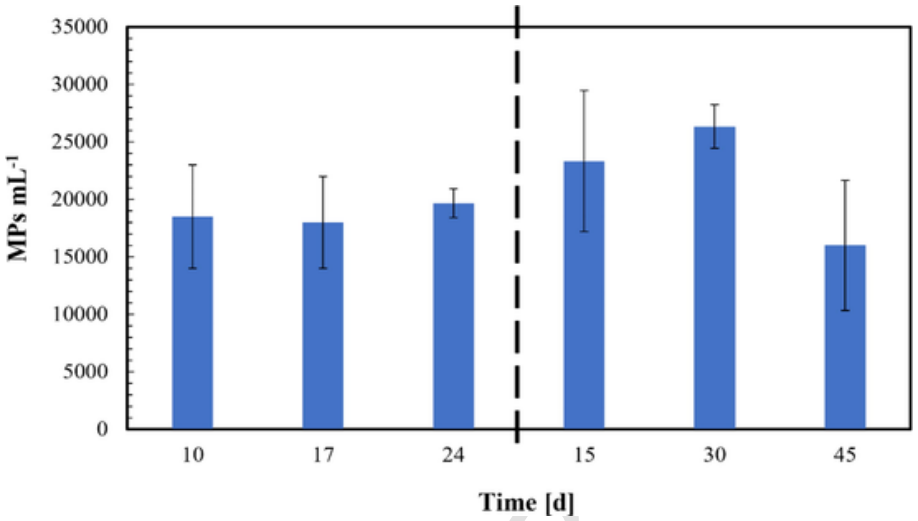

Fig. 5. The secondary microplastics concentration monitored along the biodegradation experiment. The dashed line separates the data obtained in pellets (left) and films (right).

3.5. Evolution of the plastisphere community in TPS biodegradation experiments

3.5.1. Bacterial community dynamics

The plastisphere bacterial community was monitored aiming to elucidate the key taxa involved in TPS biodegradation. The bacterial community formed was complex and varied in composition in response to biofilm and biodegradation phase (Fig. 6). Proteobacteria, Firmicutes and Actinobacteria comprised keystone taxa within TPS plastisphere at all times independently of the type of experiment conducted accounting for more than 80 % of the total community. Although proteobacteria dominated the soil TPS plastisphere (90 %), their abundance decreased in the seed community (the community established at the end of the prolonged enrichment period) and in flasks, where Firmicutes com-

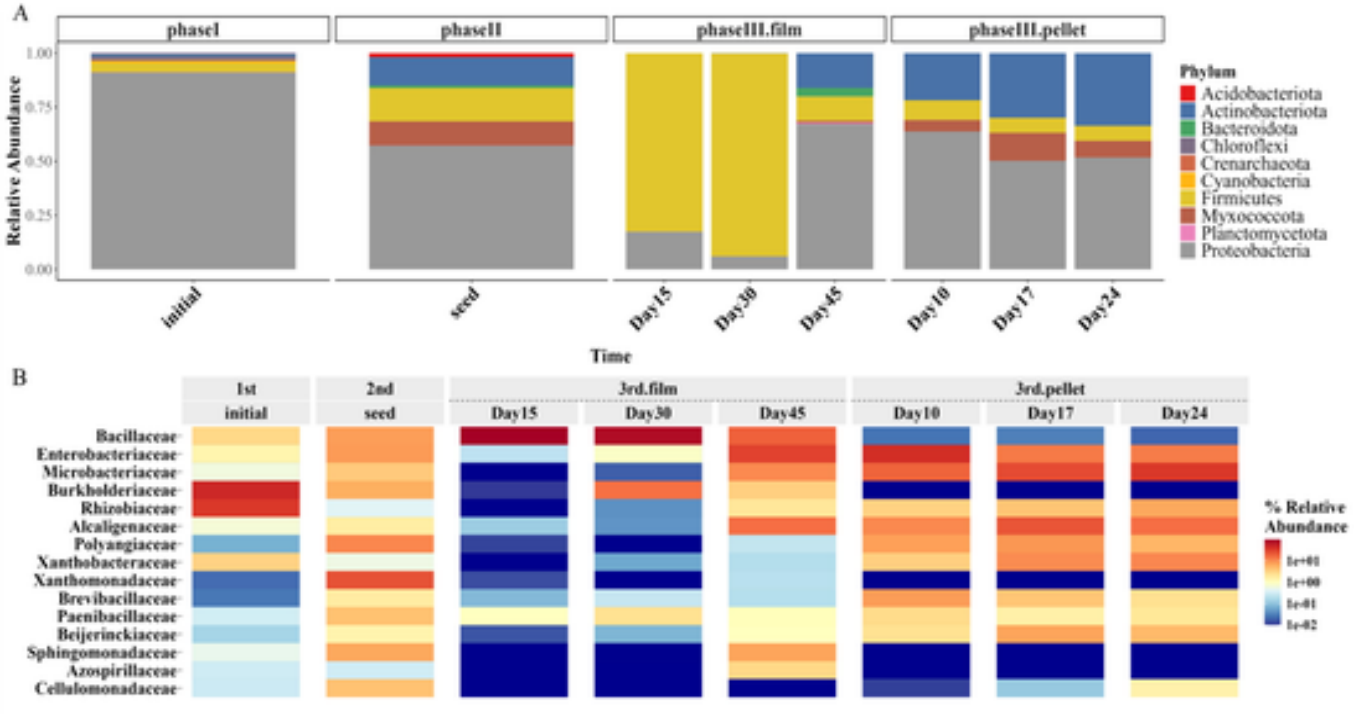

Fig. 6. The structure of bacterial communities formed within the TPS plastisphere across the different biofilm phases. (A) Relative abundance of different bacterial phyla detected within the biofilm of TPS pellets and films and (B) heatmap depicting the relative abundance of the 15 most dominant bacterial families across the biofilm phases. The phases of biofilm development are depicted (phaseI and initial: collected soil biofilm, phaseII and seed: the plastisphere at the end of the prolonged enrichment period, phaseIII.film and phaseIII.pellet: the plastisphere on the films and pellets during the biodegradation experiment where sampling days were also presented).

prised the most abundant phylum within the microorganisms attached on TPS films. Overall, community assembly dynamics in the microcosms displayed changes in ASV abundances. Specific families were enriched in attached communities depending on the phase and evolution of the biofilm. Although Burkholderiaceae and Rhizobiaceae thrived in the soil plastisphere, their abundance decreased in flasks conducting TPS biodegradation in aqueous cultures. Moreover, Microbacteriaceae and Enterobacteriaceae displayed high abundance on pellets suggesting that TPS could serve as a suitable carbon source for the growth of these microorganisms. Several genera included high abundance within the seed community and their concentration either increased or decreased during the biodegradation experiments depending on the shape of the material and the duration of incubation. Thus, statistically significant differences in the abundance of several genera were determined in the microcosms conducted, suggesting the important role of specific species in TPS biodegradation given that significant differences have been mainly monitored between the two stages of the biodegradation process (Fig. 8B). In fact, a shift from k-stategist to r-stategist taxa can be observed along the course of degradation. It is expected that oligotrophs will be the first colonizers of nutrient-poor substrates and copiotrophs will dominate in the mature and well developed (in size) community [59], while the release of TPS degradation products during the process, such as glucose and maltose, could significantly contribute to the shift observed between k-stategist and r-stategist taxa.

Microbial community diversity of all treatments was assessed via alpha diversity indices including observed species as well as Shannon and Simpson index, while the significant effect of biofilm stage was additionally monitored (Figure S3). The Shannon and Simpson index significantly increased in the plastisphere of pellets as well as during the enrichment period as compared to the soil, while high variation was monitored in the cultures conducted using films. The diversity and evenness of biofilm communities attached to TPS of both shapes increased at the plateau stage, given that higher Shannon and Simpson indices were calculated at the plateau as compared to the first stage. In the case of TPS films, the aforementioned differences were statistically significant.

NMDS was performed to visualize the patterns of attached bacterial communities along the biofilm and degradation phases, using Bray-Curtis dissimilarity (PERMANOVA, $p < 0.05$; Fig. 7A). The characteristics of the habitat formed as well as the interactions among the microorganisms contained, such as competition, promotion and symbiosis, could significantly influence the species composition, abundance and distribution [60]. Close clustering of the treatments that belonged to the same biofilm stage was observed, indicating a divergence of bacterial composition in flasks obtained from the initial soil plastisphere, while the shape of the biopolymer could be considered as an important factor for separation of the communities. Distinct biofilms assemblages were potentially formed during the TPS biodegradation process and remained different throughout the experimental period. Plastic associated communities within the natural environment tend to converge and become more similar over time [61] unless a strong weather event occurs that strongly affects community composition [62]. The relative importance of deterministic (selection) and stochastic (dispersal and other) processes in structuring the plastisphere microbial community were determined, aiming to decipher the assembly mechanisms controlling the community diversity on the different biofilm and degradation phases. Stochastic (dispersal plus drift) rather than deterministic (selection) processes potentially control the turnover. The contribution of stochastic and deterministic processes in bacterial colonization of plastics is relatively unknown, however recent studies support that stochastic processes dominate during plastisphere microbial assembly [63, 64]. Stochastic immigration and ecological drift comprise important factors in shaping prokaryotic communities, particularly within metabolic functional groups and could partly explain turnover over time in systems that involve high cell densities such as bioreactors [65]. However, the taxonomic turnover within functional groups in the absence of evident environmental variation could be driven by intrinsic and at least partly deterministic processes [65]. Thus, stochastic processes related to birth, death, colonization, extinction and speciation [66] could be important for the assembly of the communities.

Biomarkers analysis was used to determine the shared genera with significant differences in abundance among the biofilm stages (Fig. 8A).

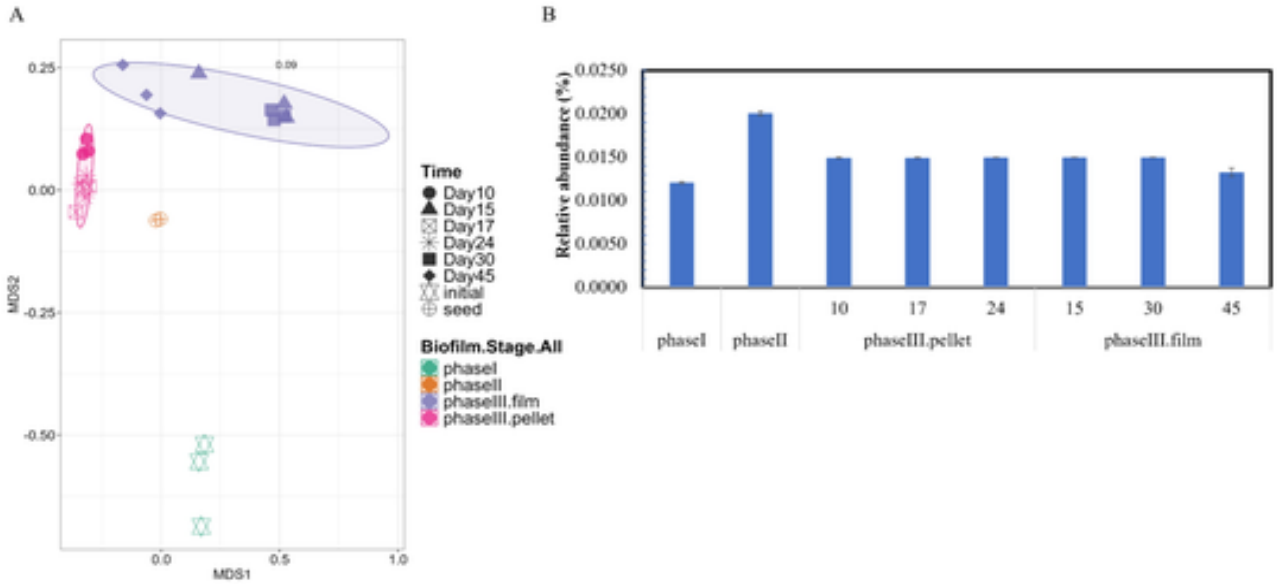

Fig. 7. The structure of bacterial communities within the TPS plastisphere. (A) NMDS ordination of Bray-Curtis distances of bacterial communities showing the separation of bacterial communities into groups based on the biofilm phase, and (B) relative abundance of the predicted pathway related to starch and sucrose metabolism in the different biofilm phases. The phases of biofilm development are depicted (1st and initial: collected soil biofilm, 2nd and seed: the plastisphere at the end of prolonged enrichment period, 3rd film and 3rd pellet: the plastisphere on the films and pellets during the biodegradation experiment where the sampling days were also presented).

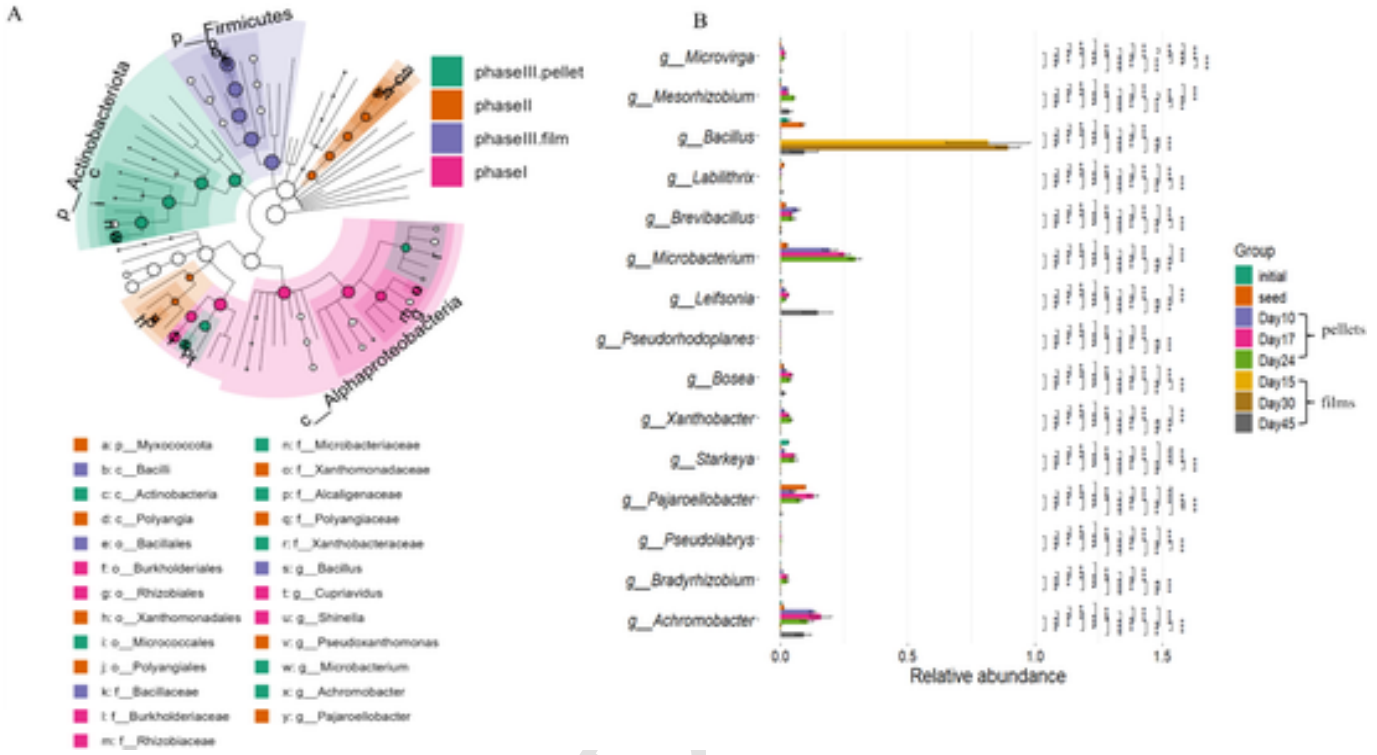

Fig. 8. The structure of bacterial communities within the TPS plastisphere. (A) Cladogram of LEfSe results according to different biofilm phases (only significant results are shown), and (B) relative abundance of the bacterial genera that differed significantly among the various biofilm phases (sampling days of the biodegradation experiment were additionally presented).

Microbacterium and *Achromobacter* played important roles in the biofilm of TPS pellets (LDA score > 4.5), while *Bacillus* was indicative in films. The specific genera have been associated with the biodegradation of biodegradable plastics in soil [67]. *Bacillus* has been characterized as starch-degrading genus and has been identified in different plastispheres including fossil-based plastics [23,68]. The presence of PLA increased the relative abundance of *Achromobacter* [69], while purified proteases and lipases from *Achromobacter* sp. have been demonstrated to hydrolyze polyesters [70].

Functional profiles of the Tax4Fun2 prediction were summarized based on KEGG pathways. Biological metabolic pathways were divided into three levels and studied along biofilm and degradation phases. Significant differences in the functional composition of the communities were determined given that certain metabolic pathways were overrepresented at specific biofilm and degradation phases. Thus, the pathway of glyoxylate and dicarboxylate metabolism was enriched within the biofilm on pellets and the pathway of amino sugar and nucleotide sugar metabolism was augmented in the biofilm of films (both belong to the carbohydrate metabolism pathway). The major predicted pathways related to carbohydrate and starch utilization were further analyzed. The pathway of starch and sucrose metabolism was indicative in seed communities, while the relative abundance of the predictive starch metabolism associated genes was monitored in the biofilm communities and significant differences were observed (Fig. 7B and Figure S4). Significantly higher abundance was detected in the seed community, while the lowest concentration was observed in soil plastisphere. During TPS degradation experiments, the relative abundance of these genes displayed a decreasing trend over time in accordance with the rate of weight reduction. Interestingly, the predictive pathways related to glycolysis/gluconeogenesis followed the same pattern. Starch could be enzymatically hydrolyzed to reducing sugars, such as maltose, maltotriose and glycose, by several enzymes including amylases and glucosidases [71]. Glucose could be further converted to pyruvic acid via glycolysis, while pyruvate dehydrogenase catalyzes the conversion of pyruvic acid to acetyl-CoA, which enters the tricarboxylic acid (TCA) cycle to produce energy and release CO_2 and water [54]. Concerning the degradation phases, increase in the relative abundance of predictive pathways related to carbohydrate metabolism such as pyruvate metabolism and TCA cycle was observed for both pellets and films along the degradation phases. Carbohydrates can alter the microbial competition, the catabolic profiles and result in the shift of the microbial community; indeed the carbohydrate metabolism selection caused a shift in the phenanthrene degrader community which further affected phenanthrene degradation [72]. A similar phenomenon was observed in our study.

3.5.2. Fungal community dynamics

The succession of the fungal community was additionally monitored given that fungi incorporate higher TPS biodegradation potential as compared to bacteria [23]. The phylum Ascomycota dominated all plastisphere communities independently of the biofilm and degradation stage (Fig. 10). Moreover, only the aforementioned phylum was detected within the attached communities developed on pellets. The saprotrophic Ascomycota have been reported as highly frequent plastic colonizers in the marine environment [73,74]. With respect to family level, *Nectriaceae* was dominant in all fungal communities, while the genera *Fusarium* and *Neocosmospora* displayed the highest abundances in all fungal assemblages (Figure S5). The fungi *Fusarium* was enriched in seed communities and within the biofilm on TPS films. However, the abundance of *Fusarium* and *Neocosmospora* in the case of pellets demonstrated inverse patterns, where *Fusarium* decreased along the degradation stages, while *Neocosmospora* increased. The fungal genus *Fusarium* includes species with well-known capacities pertinent to the production of plastic degrading enzymes such as lipase, chitinase and dehydratase

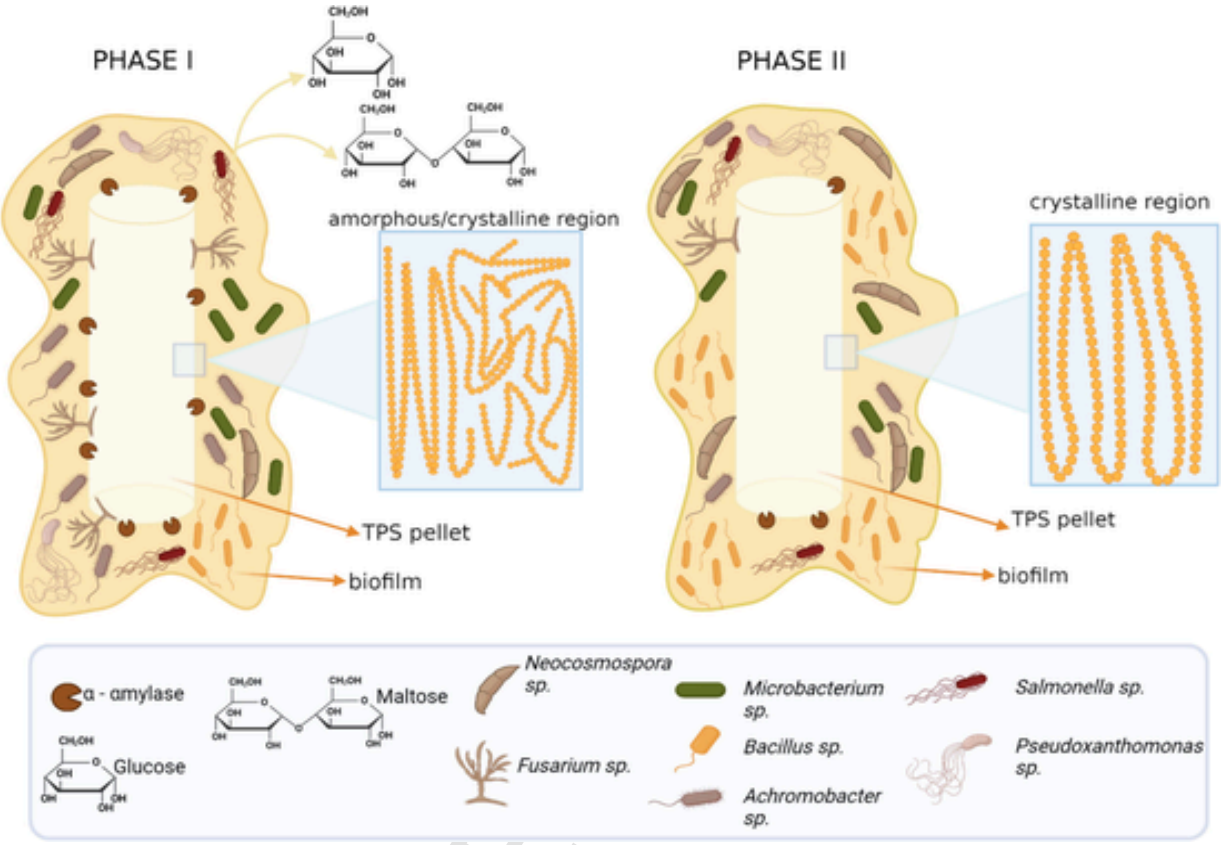

Fig. 9. The proposed bioprocess mechanism of TPS degradation (Phase I – left: the first degradation stage where the biofilm is mainly consisted of k-strategists and the polymer includes crystalline and amorphous regions; Phase II – right: the second degradation stage where r-strategists dominate the biofilm and the crystalline regions of the polymer increased over amorphous regions).

and it is considered as a promising genus in degradation of either fossil-based or biodegradable plastics [75,76]. For example, cutinase produced from *Fusarium solani* demonstrated the highest activity on grinded PBAT [77]. Moreover, members of the specific genus have been demonstrated to produce a range of carbohydrate-active enzymes (CAZymes) [78,79], which could degrade or modify polysaccharides such as cellulose, hemicelluloses and starch [80]. The genus *Neocosmospora* has been recently associated with the degradation of polycaprolactone (PCL) [81,82].

The fungal diversity along the biofilm and degradation stages was monitored using diversity indices (Figure S6). A similar pattern to the response of the bacterial community was observed. Thus, increased diversity and evenness of the fungal plastisphere along the different degradation stages was monitored, given that higher Shannon and Simpson indices were obtained at the plateau as compared to the first stage. Concerning the biofilm stages, an inverse trend was monitored as compared to the bacterial communities. The Shannon and Simpson index significantly decreased in the plastisphere during the enrichment period as compared to the soil. The fungal community developed on pellets in flasks appeared different as shown by the separate clustering in the NMDS plot (Fig. 10C). However, the specific difference was not statistically significant (PERMANOVA, $p > 0.05$). The fungal communities were more stable and there was no effect of biofilm or degradation stage on community composition, while biomarker species were not identified.

4. Conclusions

An acclimated microbial community originated from the biofilm of TPS pellets exposed to agricultural soil was isolated and used as inoculum for bioplastic biodegradation in aqueous cultures. The bioprocess displayed a two-phase pattern incorporating different biodegradation rates (Fig. 9), which remained high in the first phase (pellets: 5.8 mg d^{-1} degradation rate) and decelerated (pellets: 1.7 mg d^{-1} degradation rate) in the second phase. Although the effect of the biopolymer's shape on the biodegradation process was significant and higher weight reduction was monitored in films, the degradation pathway followed was similar. Several changes in TPS structure such as decrease of peaks, peak shifting and reduction of intensity in starch related bands were monitored during incubation. The crystalline areas formed increased along the course of the treatment potentially contributing to the lower degradation that occurred at the plateau stage. Deep surface cracks were observed on the surface of both films and pellets, while a dense biofilm was formed that completely covered TPS particles. Moreover, high content of secondary microplastics was detected in the medium due to biodegradation. Biofilm thickness slightly increased during the process and specific bacterial families were enriched in the attached communities depending on biofilm and degradation stage. Thus, the phase of biofilm formation and the shape of TPS particle comprise important factors for the separation of bacterial communities, while fungal communities did not display significant differences. A trend towards higher diversity and evenness along the degradation stages was observed for both bacteria and fungi. The genera *Microbacterium* and *Achromobacter* played important roles in the biofilm of TPS pellets and *Bacillus* was indicative in films, while the genera *Fusarium* and *Neocos-*

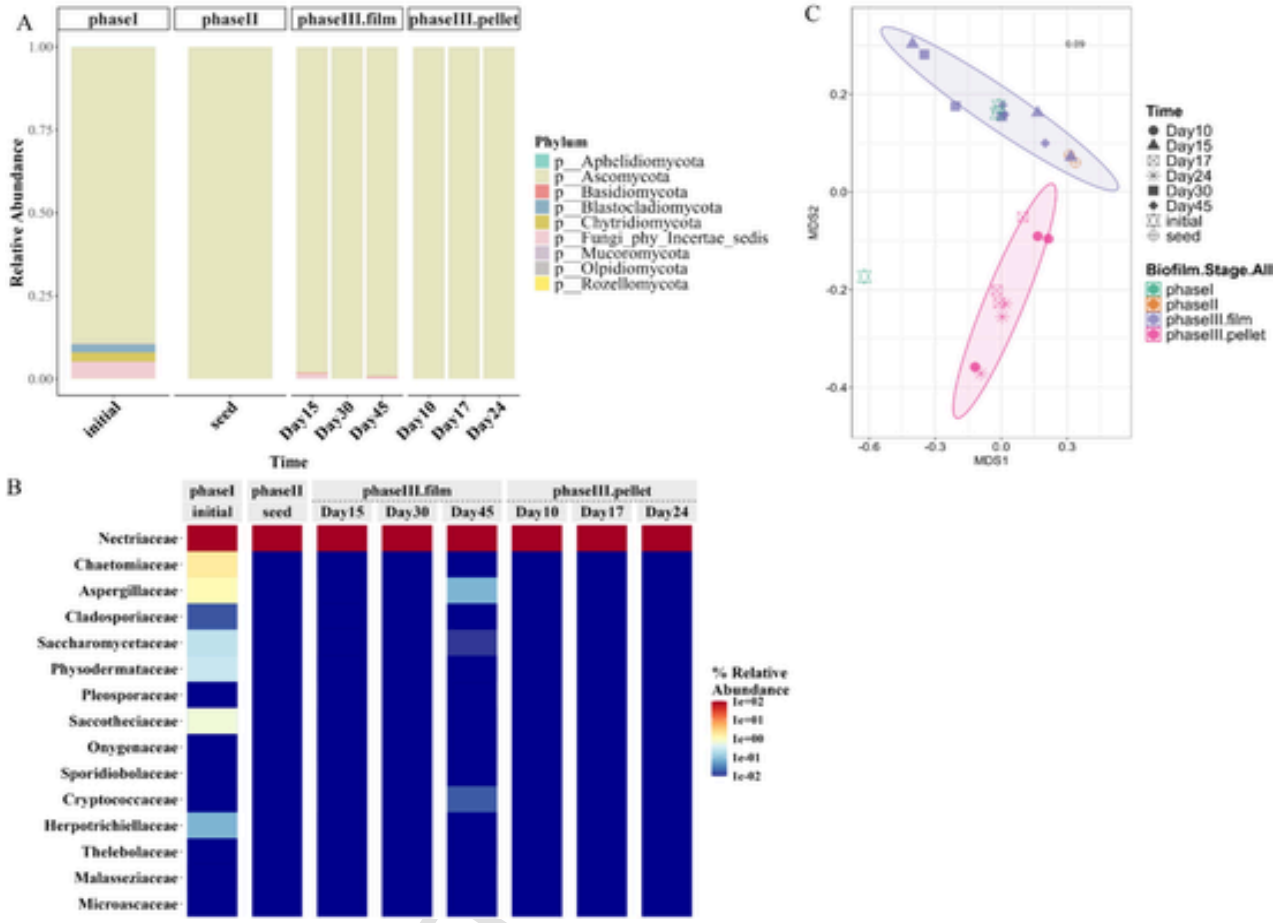

Fig. 10. Structure of fungal communities within the TPS plastisphere. (A) Relative abundance of fungal phyla in the different biofilm phases, (B) heatmap demonstrating the relative abundance of the top 15 fungal families in the different biofilm phases, and (C) NMDS ordination of Bray-Curtis distances of fungal communities.

mospora displayed the highest abundance in all fungal assemblages. A shift from k-stategist to r-stategist taxa was monitored during the experiments suggesting that the mode of biodegradation followed included oligotrophs as the first colonizers of TPS followed by copiotrophs dominating the mature community potentially due to the release of easy metabolizable TPS degradation products (e.g. glucose, maltose). Overall, this is the first study to our knowledge assessing the efficiency of an acclimated biofilm community for TPS biodegradation under mesophilic conditions using aqueous cultures. Results demonstrated the significant potential for TPS waste treatment in an industrial environment as compared to composting and anaerobic digestion, unraveling the microbial mechanisms underlying the reduction in bioprocess performance. Future research should focus on tackling the reduction of biodegradation rate at the plateau stage.

CRediT authorship contribution statement

Evdokia Syranidou: Writing – original draft, Methodology, Funding acquisition, Formal analysis, Data curation, Conceptualization. **Fryni Pyrilli:** Writing – original draft, Methodology, Investigation, Formal analysis, Data curation. **Athanasios Fountoulakis:** Investigation, Data curation. **Georgios Constantinides:** Writing – review & editing, Resources, Methodology, Investigation. **Nicolas Kalogerakis:** Writing – review & editing, Supervision, Resources. **Michalis Koutinas:** Writing – review & editing, Supervision, Resources, Methodology, Funding acquisition, Conceptualization.

Declaration of competing interest

The authors declare the following financial interests/personal relationships which may be considered as potential competing interests: Michalis Koutinas reports financial support was provided by Horizon 2020 Framework Programme H2020. If there are other authors, they declare that they have no known competing financial interests or personal relationships that could have appeared to influence the work reported in this paper.

Acknowledgements

This work was supported by the Horizon 2020 Framework Programme H2020 – MSCA/ERA-IF-Postdoctoral Fellowships - 2021 [grant number 101065005].

Data availability

Data will be made available on request.

Appendix A. Supplementary data

Supplementary data to this article can be found online at https://doi.org/10.1016/j.cej.2024.155957.

References

[1] J.M. Millican, S. Agarwal, Plastic pollution: a material problem? Macromolecules 54 (2021) 4455–4469, https://doi.org/10.1021/acs.macromol.0c02814.

[2] D. Klingelhöfer, M. Braun, D. Quarcoo, D. Brüggmann, D.A. Groneberg, Research landscape of a global environmental challenge: microplastics, Water Res. 170 (2020) 115358, https://doi.org/10.1016/j.watres.2019.115358.

[3] O.S. Alimi, D. Claveau-Mallet, R.S. Kurusu, M. Lapointe, S. Bayen, N. Tufenkji, Weathering pathways and protocols for environmentally relevant microplastics and nanoplastics: what are we missing? J. Hazard. Mater. 423 (2022) 126955, https://doi.org/10.1016/j.jhazmat.2021.126955.

[4] J. Oliveira, A. Belchior, V.D. da Silva, A. Rotter, Ž. Petrovski, P.L. Almeida, N.D. Lourenço, S.P. Gaudêncio, Marine environmental plastic pollution: Mitigation by microorganism degradation and recycling valorization, Front. Mar. Sci. 7 (2020) 567126, https://doi.org/10.3389/fmars.2020.567126.

[5] P.S. Calabrò, M. Grosso, Bioplastics and waste management, Waste Manag. 78 (2018) 800–801, https://doi.org/10.1016/j.wasman.2018.06.054.

[6] G. Bishop, D. Styles, P.N.L. Lens, Environmental performance comparison of bioplastics and petrochemical plastics: a review of life cycle assessment (LCA) methodological decisions, Resour. Conserv. Recycl. 168 (2021) 105451, https://doi.org/10.1016/j.resconrec.2021.105451.

[7] P.T. Benavides, U. Lee, O. Zare-Mehrjerdi, Life cycle greenhouse gas emissions and energy use of polylactic acid, bio-derived polyethylene, and fossil-derived polyethylene, J. Clean. Prod. 277 (2020) 124010, https://doi.org/10.1016/j.jclepro.2020.124010.

[8] M. Cucina, P. De Nisi, F. Tambone, F. Adani, The role of waste management in reducing bioplastics' leakage into the environment: a review, Bioresour. Technol. 337 (2021) 125459, https://doi.org/10.1016/j.biortech.2021.125459.

[9] M. Shen, B. Song, G. Zeng, Y. Zhang, W. Huang, X. Wen, W. Tang, Are biodegradable plastics a promising solution to solve the global plastic pollution? Environ. Pollut. 263 (2020) 114469, https://doi.org/10.1016/j.envpol.2020.114469.

[10] S. Spierling, V. Venkatachalam, M. Mudersbach, N. Becker, C. Herrmann, H.J. Endres, End-of-life options for bio-based plastics in a circular economy-status quo and potential from a life cycle assessment perspective, Resources. 9 (2020) 90, https://doi.org/10.3390/RESOURCES9070090.

[11] T.P. Haider, C. Völker, J. Kramm, K. Landfester, F.R. Wurm, Plastics of the Future? The impact of biodegradable polymers on the environment and on society, Angew. Chemie - Int. Ed. 58 (2019) 50–62, https://doi.org/10.1002/anie.201805766.

[12] A. Nandakumar, J.A. Chuah, K. Sudesh, Bioplastics: a boon or bane? Renew. Sustain. Energy Rev. 147 (2021) 111237, https://doi.org/10.1016/j.rser.2021.111237.

[13] X. Zhao, K. Cornish, Y. Vodovotz, Narrowing the gap for bioplastic use in food packaging: an update, Environ. Sci Technol. 54 (2020) 4712–4732, https://doi.org/10.1021/acs.est.9b03755.

[14] A.R. Bergeson, A.J. Silvera, H.S. Alper, Bottlenecks in biobased approaches to plastic degradation, Nat. Commun. 15 (2024) 1–9, https://doi.org/10.1038/s41467-024-49146-8.

[15] R. Kumar, K. Sadeghi, J. Jang, J. Seo, Mechanical, chemical, and bio-recycling of biodegradable plastics: a review, Sci. Total Environ. 882 (2023) 163446, https://doi.org/10.1016/j.scitotenv.2023.163446.

[16] E.C. Van Roijen, S.A. Miller, A review of bioplastics at end-of-life: Linking experimental biodegradation studies and life cycle impact assessments, Resour. Conserv. Recycl. 181 (2022) 106236, https://doi.org/10.1016/j.resconrec.2022.106236.

[17] V.C. Shruti, G. Kutralam-Muniasamy, Bioplastics: missing link in the era of microplastics, Sci. Total Environ. 697 (2019) 134139, https://doi.org/10.1016/j.scitotenv.2019.134139.

[18] G. Cazaudehore, F. Monlau, C. Gassie, A. Lallement, R. Guyoneaud, Active microbial communities during biodegradation of biodegradable plastics by mesophilic and thermophilic anaerobic digestion, J. Hazard. Mater. 443 (2023) 130208, https://doi.org/10.1016/j.jhazmat.2022.130208.

[19] A. Morro, F. Catalina, T. Corrales, J.L. Pablos, I. Marin, C. Abrusci, New blends of ethylene-butyl acrylate copolymers with thermoplastic starch. Characterization and bacterial biodegradation, Carbohydr. Polym. 149 (2016) 68–76, https://doi.org/10.1016/j.carbpol.2016.04.075.

[20] T. Narancic, S. Verstichel, S. Reddy Chaganti, L. Morales-Gamez, S.T. Kenny, B. De Wilde, R. Babu Padamati, K.E. O'Connor, Biodegradable plastic blends create new possibilities for End-of-Life management of plastics but they are not a panacea for plastic pollution, Environ. Sci. Technol. 52 (2018) 10441–10452, https://doi.org/10.1021/acs.est.8b02963.

[21] R. Iovino, R. Zullo, M.A. Rao, L. Cassar, L. Gianfreda, Biodegradation of poly (lactic acid)/ starch / coir biocomposites under controlled composting conditions, Polym. Degrad. Stab. 93 (2008) 147–157, https://doi.org/10.1016/j.polymdegradstab.2007.10.011.

[22] A. Folino, A. Karageorgiou, P.S. Calabrò, D. Komilis, Biodegradation of wasted bioplastics in natural and industrial environments: a review, Sustainability 12 (2020) 1–37, https://doi.org/10.3390/su12156030.

[23] E.M.N. Polman, G.J.M. Gruter, J.R. Parsons, A. Tietema, Comparison of the aerobic biodegradation of biopolymers and the corresponding bioplastics: a review, Sci. Total Environ. 753 (2021) 141953, https://doi.org/10.1016/j.scitotenv.2020.141953.

[24] A.K. Urbanek, W. Rymowicz, M.C. Strzelecki, W. Kociuba, Ł. Franczak, A.M. Mirończuk, Isolation and characterization of arctic microorganisms decomposing bioplastics, AMB Express. 7 (2017) 148, https://doi.org/10.1186/s13568-017-0448-4.

[25] D. Lobelle, M. Cunliffe, Early microbial biofilm formation on marine plastic debris, Mar. Pollut. Bull. 62 (2011) 197–200, https://doi.org/10.1016/j.marpolbul.2010.10.013.

[26] N.L. Tai, R. Adhikari, R. Shanks, B. Adhikari, Aerobic biodegradation of starch – polyurethane flexible films under soil burial condition: changes in physical structure and chemical composition, Int. Biodeterior. Biodegrad. 145 (2019) 104793, https://doi.org/10.1016/j.ibiod.2019.104793.

[27] V.M. Moo-Huchin, M.J. Cabrera-Sierra, R.J. Estrada-Leon, C.R. Ríos-Soberanis, D. Betancur-Ancona, L. Chel-Guerrero, A. Ortiz-Fernandez, I.A. Estrada-Mota, E. Perez-Pacheco, Determination of some physicochemical and rheological characteristics of starch obtained from Brosimum alicastrum swartz seeds, Food Hydrocoll. 45 (2015) 48–54, https://doi.org/10.1016/j.foodhyd.2014.11.009.

[28] M. Martin, Cutadapt removes adapter sequences from high-throughput sequencing reads, EMBnet J. 17 (2011) 10–12, https://doi.org/10.14806/ej.17.1.200.

[29] B.J. Callahan, P.J. McMurdie, M.J. Rosen, A.W. Han, A.J.A. Johnson, S.P. Holmes, DADA2: high-resolution sample inference from Illumina amplicon data, Nat. Methods. 13 (2016) 581–583, https://doi.org/10.1038/nmeth.3869.

[30] C. Quast, E. Pruesse, P. Yilmaz, J. Gerken, T. Schweer, P. Yarza, J. Peplies, F.O. Glöckner, The SILVA ribosomal RNA gene database project: improved data processing and web-based tools, Nucleic Acids Res. 41 (2013) 590–596, https://doi.org/10.1093/nar/gks1219.

[31] R.H. Nilsson, K.H. Larsson, A.F.S. Taylor, J. Bengtsson-Palme, T.S. Jeppesen, D. Schigel, P. Kennedy, K. Picard, F.O. Glöckner, L. Tedersoo, I. Saar, U. Kõljalg, K. Abarenkov, The UNITE database for molecular identification of fungi: handling dark taxa and parallel taxonomic classifications, Nucleic Acids Res. 47 (2019) D259–D264, https://doi.org/10.1093/nar/gky1022.

[32] E.S. Wright, Using DECIPHER v2.0 to analyze big biological sequence data in R, R J. 8 (2016) 352–359. https://doi.org/10.32614/rj-2016-025.

[33] K.P. Schliep, phangorn: phylogenetic analysis in R, Bioinformatics. 27 (2011) 592–593, https://doi.org/10.1093/bioinformatics/btq706.

[34] C. Liu, Y. Cui, X. Li, M. Yao, Microeco: an R package for data mining in microbial community ecology, FEMS Microbiol. Ecol. 97 (2021) 1–9, https://doi.org/10.1093/femsec/fiaa255.

[35] J. Oksanen, F.G. Blanchet, Michael Friendly, R. Kindt, P. Legendre, P. Dan McGlinn, R. Minchin, R.B. O'Hara, G.L. Simpson, P. Solymos, M.H.H. Stevens, E. Szoecs, H. Wagner, P. Legendre, B. O'Hara, M.H.H. Stevens, M.J. Oksanen, M. Suggests, T Package 'Vegan'. Community Ecology Package, Version 2. Available at: http://CRAN.R-project.org/package=vegan.

[36] N. Segata, J. Izard, L. Waldron, D. Gevers, L. Miropolsky, W.S.W. Garrett, C. Huttenhower, Metagenomic biomarker discovery and explanation, Genome Biol. 12 (2011) R60, https://doi.org/10.1186/gb-2011-12-6-r60.

[37] J.R. White, N. Nagarajan, M. Pop, Statistical methods for detecting differentially abundant features in clinical metagenomic samples, PLoS Comput. Biol. 5 (2009) e1000352.

[38] F. Wemheuer, J.A. Taylor, R. Daniel, E. Johnston, P. Meinicke, T. Thomas, Tax4Fun2: prediction of habitat-specific functional profiles and functional redundancy based on 16S rRNA gene sequences, Environ. Microbiome. 7 (2020) 1–12.

[39] P.J. McMurdie, S. Holmes, Phyloseq: an R package for reproducible interactive analysis and graphics of microbiome census data, PLoS One 8 (2013) e61217, https://doi.org/10.1371/journal.pone.0061217.

[40] T.T. Duong, P.T. Le, T.N.H. Nguyen, T.Q. Hoang, H.M. Ngo, T.O. Doan, T.P.Q. Le, H.T. Bui, M.H. Bui, V.T. Trinh, T.L. Nguyen, N. Da Le, T.M. Vu, T.K.C. Tran, T.C. Ho, N.N. Phuong, E. Strady, Selection of a density separation solution to study microplastics in tropical riverine sediment, Environ. Monit. Assess. 194 (2022) 65, https://doi.org/10.1007/s10661-021-09664-0.

[41] G. Erni-Cassola, M.I. Gibson, R.C. Thompson, J.A. Christie-Oleza, Lost, but Found with Nile Red: a novel method for detecting and quantifying small microplastics (1 mm to 20 μm) in environmental samples, Environ. Sci. Technol. 51 (2017) 13641–13648, https://doi.org/10.1021/acs.est.7b04512.

[42] Y. Du, Y. Cao, F. Lu, F. Li, Y. Cao, X. Wang, Y. Wang, Biodegradation behaviors of thermoplastic starch (TPS) and thermoplastic dialdehyde starch (TPDAS) under controlled composting conditions, Polym. Test. 27 (2008) 924–930, https://doi.org/10.1016/j.polymertesting.2008.08.002.

[43] F.G. Torres, O.P. Troncoso, C. Torres, D.A. Díaz, E. Amaya, Biodegradability and mechanical properties of starch films from Andean crops, Int. J. Biol. Macromol. 48 (2011) 603–606, https://doi.org/10.1016/j.ijbiomac.2011.01.026.

[44] S.V. Afshar, A. Boldrin, T.F. Astrup, A.E. Daugaard, N.B. Hartmann, Degradation of biodegradable plastics in waste management systems and the open environment: a critical review, J. Clean. Prod. 434 (2024) 140000, https://doi.org/10.1016/j.jclepro.2023.140000.

[45] M. Ghasemlou, F. Daver, B.J. Murdoch, A.S. Ball, E.P. Ivanova, B. Adhikari, Biodegradation of novel bioplastics made of starch, polyhydroxyurethanes and cellulose nanocrystals in soil environment, Sci. Total Environ. 815 (2022) 152684, https://doi.org/10.1016/j.scitotenv.2021.152684.

[46] Q. Feng, C. An, Z. Chen, J. Yin, B. Zhang, K. Lee, Z. Wang, Investigation into the impact of aged microplastics on oil behavior in shoreline environments, J. Hazard. Mater. 421 (2022) 126711, https://doi.org/10.1016/j.jhazmat.2021.126711.

[47] K.G. Ho, I.A.L. Pometto, Temperature effects on soil mineralization of polylactic acid plastic in laboratory respirometers, J. Environ. Polym. Degrad. 7 (1999) 101–108, https://doi.org/10.1023/A:1021812418325.

[48] M. Haslam, The decomposition of starch grains in soils: implications for archaeological residue analyses, J. Archaeol. Sci. 31 (2004) 1715–1734, https://

doi.org/10.1016/j.jas.2004.05.006.
[49] S.K. Awasthi, M. Kumar, V. Kumar, S. Sarsaiya, P. Anerao, P. Ghosh, L. Singh, H. Liu, Z. Zhang, M.K. Awasthi, A comprehensive review on recent advancements in biodegradation and sustainable management of biopolymers, Environ. Pollut. 307 (2022) 119600, https://doi.org/10.1016/j.envpol.2022.119600.
[50] P. Tyagi, S. Agate, O.D. Velev, L. Lucia, L. Pal, A critical review of the performance and soil biodegradability profiles of biobased natural and chemically synthesized polymers in industrial applications, Environ. Sci. Technol. 56 (2022) 2071–2095, https://doi.org/10.1021/acs.est.1c04710.
[51] A. Sankri, A. Arhaliass, I. Dez, A. Claude, Y. Grohens, D. Lourdin, I. Pillin, A. Rolland-sabaté, E. Leroy, Thermoplastic starch plasticized by an ionic liquid, Carbohydr. Polym. 82 (2010) 256–263, https://doi.org/10.1016/j.carbpol.2010.04.032.
[52] S. Pokhrel, A. Sigdel, R. Lach, M. Slouf, J. Sirc, D.R. Bhattarai, R. Adhikari, Starch-based biodegradable film with preparation, morphology, thermal and biodegradation properties, J. Macromol. Sci. Part A. 58 (2021) 610–621, https://doi.org/10.1080/10601325.2021.1920838.
[53] C.A. Rodrigues, A. Tofanello, I.L. Nantes, D.S. Rosa, Biological oxidative mechanisms for degradation of poly(lactic acid) blended with thermoplastic starch, ACS Sustain. Chem. Eng. 3 (2015) 2756–2766, https://doi.org/10.1021/acssuschemeng.5b00639.
[54] A. Bher, P.C. Mayekar, R.A. Auras, Biodegradation of biodegradable polymers in mesophilic aerobic environments, Int. J. Mol. Sci. 23 (2022) 12165, https://doi.org/10.3390/ijms232012165.
[55] E. Syranidou, K. Karkanorachaki, D. Barouta, E. Papadaki, D. Moschovas, A. Avgeropoulos, N. Kalogerakis, Relationship between the carbonyl index (CI) and fragmentation of polyolefin plastics during aging, Environ. Sci. Technol. 57 (2023) 8130–8138, https://doi.org/10.1021/acs.est.3c01430.
[56] A.L. Andrady, Weathering and fragmentation of plastic debris in the ocean environment, Mar. Pollut. Bull. 180 (2022) 113761, https://doi.org/10.1016/j.marpolbul.2022.113761.
[57] S. Agarwal, Biodegradable polymers: present opportunities and challenges in providing a microplastic-free environment, Macromol. Chem. Phys. 221 (2020) 2000017, https://doi.org/10.1002/macp.202000017.
[58] X.F. Wei, M. Bohlén, C. Lindblad, M. Hedenqvist, A. Hakonen, Microplastics generated from a biodegradable plastic in freshwater and seawater, Water Res. 198 (2021) 117123, https://doi.org/10.1016/j.watres.2021.117123.
[59] N. Fierer, M.A. Bradford, R.B. Jackson, Toward an ecological classification of soil bacteria, Ecology 88 (2007) 1354–1364, https://doi.org/10.1890/05-1839.
[60] Z. Li, C. Feng, J. Lei, X. He, Q. Wang, Y. Zhao, Y. Qian, X. Zhan, Z. Shen, Farmland Microhabitat mediated by a residual microplastic film: microbial communities and function, Environ. Sci. Technol. 58 (2024) 3654–3664, https://doi.org/10.1021/acs.est.3c07717.
[61] S. Martínez-Campos, M. González-Pleiter, A. Rico, T. Schell, M. Vighi, F. Fernández-Piñas, R. Rosal, F. Leganés, Time-course biofilm formation and presence of antibiotic resistance genes on everyday plastic items deployed in river waters, J. Hazard. Mater. 443 (2023) 130271, https://doi.org/10.1016/j.jhazmat.2022.130271.
[62] K. Karkanorachaki, E. Syranidou, N. Kalogerakis, Extreme weather events as an important factor for the evolution of plastisphere but not for the degradation process, Water Res. 246 (2023) 120687, https://doi.org/10.1016/j.watres.2023.120687.
[63] S.J. Zhang, Y.H. Zeng, J.M. Zhu, Z.H. Cai, J. Zhou, The structure and assembly mechanisms of plastisphere microbial community in natural marine environment, J. Hazard. Mater. 421 (2022) 126780, https://doi.org/10.1016/j.jhazmat.2021.126780.
[64] L.Y. Yang, X.R. Huang, R. Neilson, S.Y.D. Zhou, Z.L. Li, X.R. Yang, X.X. Su, Characterization of microbial community, ecological functions and antibiotic resistance in estuarine plastisphere, Sci. Total Environ. 866 (2023) 161322, https://doi.org/10.1016/j.scitotenv.2022.161322.
[65] S. Louca, M.F. Polz, F. Mazel, M.B.N. Albright, J.A. Huber, M.I. O'Connor, M. Ackermann, A.S. Hahn, D.S. Srivastava, S.A. Crowe, M. Doebeli, L.W. Parfrey, Function and functional redundancy in microbial systems, Nat. Ecol. Evol. 2 (2018) 936–943, https://doi.org/10.1038/s41559-018-0519-1.
[66] W. Xun, W. Li, W. Xiong, Y. Ren, Y. Liu, Y. Miao, Z. Xu, N. Zhang, Q. Shen, R. Zhang, Diversity-triggered deterministic bacterial assembly constrains community functions, Nat. Commun. 10 (2019) 3833, https://doi.org/10.1038/s41467-019-11787-5.
[67] Y. Zhou, M. Kumar, S. Sarsaiya, R. Sirohi, S.K. Awasthi, R. Sindhu, P. Binod, A. Pandey, N.S. Bolan, Z. Zhang, L. Singh, S. Kumar, M.K. Awasthi, Challenges and opportunities in bioremediation of micro-nano plastics: a review, Sci. Total Environ. 802 (2022) 149823, https://doi.org/10.1016/j.scitotenv.2021.149823.
[68] R.M.M. Abed, M. Al-Hinai, Y. Al-Balushi, L. Haider, T. Muthukrishnan, U. Rinner, Degradation of starch-based bioplastic bags in the pelagic and benthic zones of the Gulf of Oman, Mar. Pollut. Bull. 195 (2023) 115496, https://doi.org/10.1016/j.marpolbul.2023.115496.
[69] A.N. Mistry, B. Kachenchart, A. Wongthanaroj, A. Somwangthanaroj, E. Luepromchai, Rapid biodegradation of high molecular weight semi-crystalline polylactic acid at ambient temperature via enzymatic and alkaline hydrolysis by a defined bacterial consortium, Polym. Degrad. Stab. 202 (2022) 110051, https://doi.org/10.1016/j.polymdegradstab.2022.110051.
[70] M. Hajighasemi, A. Tchigvintsev, B. Nocek, R. Flick, A. Popovic, T. Hai, A.N. Khusnutdinova, G. Brown, X. Xu, H. Cui, J. Anstett, T.N. Chernikova, T. Bru, D. Le Paslier, M.M. Yakimov, A. Joachimiak, O.V. Golyshina, A. Savchenko, P.N. Golyshin, E.A. Edwards, A.F. Yakunin, Screening and characterization of novel polyesterases from environmental metagenomes with high hydrolytic activity against synthetic polyesters, Environ. Sci. Technol. (2018) 12388–12401, https://doi.org/10.1021/acs.est.8b04252.
[71] M.S. Møller, B. Svensson, Structural biology of starch-degrading enzymes and their regulation, Curr. Opin. Struct. Biol. 40 (2016) 33–42, https://doi.org/10.1016/j.sbi.2016.07.006.
[72] L. Jiang, C. Luo, D. Zhang, M. Song, W. Mei, Y. Sun, G. Zhang, Shifts in a phenanthrene-degrading microbial community are driven by carbohydrate metabolism selection in a ryegrass rhizosphere, Environ. Sci. Technol. 55 (2021) 962–973, https://doi.org/10.1021/acs.est.0c04951.
[73] C. De Tender, L.I. Devriese, A. Haegeman, S. Maes, J. Vangeyte, A. Cattrijsse, P. Dawyndt, T. Ruttink, Temporal dynamics of bacterial and fungal colonization on plastic debris in the North Sea, Environ. Sci. Technol. 51 (2017) 7350–7360, https://doi.org/10.1021/acs.est.7b00697.
[74] A.L.d.F. Lacerda, M.C. Proietti, E.R. Secchi, J.D. Taylor, Diverse groups of fungi are associated with plastics in the surface waters of the Western South Atlantic and the Antarctic Peninsula, Mol. Ecol. 29 (2020) 1903–1918, https://doi.org/10.1111/mec.15444.
[75] V. Guliyev, B. Tanunchai, M. Noll, F. Buscot, W. Purahong, E. Blagodatskaya, Links among microbial communities, soil properties and functions: are fungi the sole players in decomposition of bio-based and biodegradable plastic? Polymers (basel). 14 (2022) 2801, https://doi.org/10.3390/polym14142801.
[76] V.M. Pathak, Navneet, Review on the current status of polymer degradation: a microbial approach, Bioresour. Bioprocess. 4 (2017) 15, https://doi.org/10.1186/s40643-017-0145-9.
[77] F. Santos-Beneit, L.M. Chen, S. Bordel, R. Frutos de la Flor, O. García-Depraect, R. Lebrero, S. Rodriguez-Vega, R. Muñoz, R.A. Börner, T. Börner, Screening enzymes that can depolymerize commercial biodegradable polymers: Heterologous expression of fusarium solani cutinase in *Escherichia coli*, Microorganisms 11 (2023) 328, https://doi.org/10.3390/microorganisms11020328.
[78] D. Chettri, A.K. Verma, A.K. Verma, Innovations in CAZyme gene diversity and its modification for biorefinery applications, Biotechnol. Rep. 28 (2020) e00525, https://doi.org/10.1016/j.btre.2020.e00525.
[79] S.C. Brandt, H. Brognaro, A. Ali, B. Ellinger, K. Maibach, M. Rühl, C. Wrenger, H. Schlüter, W. Schäfer, C. Betzel, S. Janssen, M. Gand, Insights into the genome and secretome of *Fusarium metavorans* DSM105788 by cultivation on agro-residual biomass and synthetic nutrient sources, Biotechnol. Biofuels. 14 (2021) 1–22, https://doi.org/10.1186/s13068-021-01927-9.
[80] C. Filiatrault-Chastel, S. Heiss-Blanquet, A. Margeot, J.G. Berrin, From fungal secretomes to enzymes cocktails: the path forward to bioeconomy, Biotechnol. Adv. 52 (2021) 107833, https://doi.org/10.1016/j.biotechadv.2021.107833.
[81] G. Pang, X. Li, M. Ding, S. Jiang, P. Chen, Z. Zhao, R. Gao, B. Song, X. Xu, Q. Shen, F.M. Cai, I.S. Druzhinina, The distinct plastisphere microbiome in the terrestrial-marine ecotone is a reservoir for putative degraders of petroleum-based polymers, J. Hazard. Mater. 453 (2023) 131399, https://doi.org/10.1016/j.jhazmat.2023.131399.
[82] A.S. Al, J.K. Pittman, G.D. Robson, Microbial degradation of four biodegradable polymers in soil and compost demonstrating polycaprolactone as an ideal compostable plastic, Waste Manag. 97 (2019) 105–114, https://doi.org/10.1016/j.wasman.2019.07.042.